Automatic Extraction of Recurrent Patterns of High Dominant Frequency Mapping during Human Persistent Atrial Fibrillation

Xin Li[1, 2*], Gavin S. Chu[2], Tiago P. Almeida[2, 1], Frederique J. Vanheusden[3], João Salinet[4], Nawshin Dastagir[5], Amar R. Mistry[2], Zakariyya Vali[2, 6], Bharat Sidhu[2], Peter J. Stafford[6], Fernando S. Schlindwein[1, 6], G. Andre Ng[2, 6]

[1]School of Engineering, University of Leicester, United Kingdom, [2]Department of Cardiovascular Sciences, University of Leicester, United Kingdom, [3]School of Science and Technology, Nottingham Trent University, United Kingdom, [4]Center of Engineering, Modelling and Applied Social Sciences, Federal University of ABC, Brazil, [5]Auckland Bioengineering Institute, University of Auckland, New Zealand, [6]NIHR Leicester Biomedical Research Centre, United Kingdom

Submitted to Journal:
Frontiers in Physiology

Specialty Section:
Cardiac Electrophysiology

Article type:
Original Research Article

Manuscript ID:
649486

Received on:
04 Jan 2021

Revised on:
19 Feb 2021

Journal website link:
www.frontiersin.org

Conflict of interest statement

The authors declare a potential conflict of interest and state it below

Professor Ng has received a research fellowship from St. Jude Medical (now Abbott) and speaker fees and honoraria from Biosense Webster. All other authors have reported that they have no relationships relevant to the contents of this paper to disclose.

Author contribution statement

Contribution of each co-author to the submitted work
• Xin Li: concept/design study, data analysis/interpretation of results, drafting manuscript, critical revision of manuscript, statistics, and 'off-line' data collection;
• Gavin S. Chu: concept/design study, data analysis/interpretation of results, drafting manuscript, critical revision of manuscript, statistics, and 'off-line' data collection;
• Tiago P. Almeida: data analysis/interpretation of results, drafting manuscript, critical revision of manuscript, statistics;
• Frederique J Vanheusden: data analysis/interpretation of results, critical revision of manuscript, statistics;
• João Salinet: data analysis/interpretation of results, critical revision of manuscript;
• Nawshin Dastagir: data analysis/interpretation of results, critical revision of manuscript, statistics;
• Amar R Mistry: data analysis/interpretation of results, critical revision of manuscript;
• Zakariyya Vali: data analysis/interpretation of results, critical revision of manuscript, statistics;
• Bharat Sidhu: data analysis/interpretation of results, critical revision of manuscript, statistics;
• Peter J. Stafford: EP study, data collection, interpretation of results, critical revision of manuscript;
• Fernando S. Schlindwein: Concept/design study, data analysis, interpretation of results, critical revision of manuscript;
• G. André Ng: EP studies and ablation procedures, concept/design study, interpretation of results, critical revision of manuscript.

Keywords

Atrial Fibrillation, catheter ablation – atrial fibrillation, Non-contact mapping, Atrial electrograms (EGMs), Dominant Frequency Analyses, Recurrent Patterns, spatiotemporal patterns, pattern recognition

Abstract

Word count: 350

Purpose: Identifying targets for catheter ablation remains challenging in persistent atrial fibrillation (persAF). The dominant frequency (DF) of atrial electrograms during atrial fibrillation (AF) is believed to primarily reflect local activation. Highest DF (HDF) might be responsible for the initiation and perpetuation of persAF. However, the spatiotemporal behaviour of DF remains not fully understood. Some DFs during persAF were shown to lack spatiotemporal stability, while others exhibit recurrent behaviour. We sought to develop a tool to automatically detect recurrent DF patterns in persAF patients.
Methods: Non-contact mapping of the left atrium (LA) was performed in 10 patients undergoing persAF HDF ablation. 2048 virtual electrograms (vEGMs, EnSite Array, Abbott Laboratories, USA) were collected for up to 5 min before and after ablation. Frequency spectrum was estimated using fast Fourier transform and DF was identified as the peak between 4-10 Hz and organization index (OI) was calculated. The HDF maps were identified per 4-second window and an automated pattern recognition algorithm was used to find recurring HDF spatial patterns. Dominant patterns (DPs) were defined as the HDF pattern with the highest recurrence.
Results: DPs were found in all patients. Patients in atrial flutter after ablation had a single DP over the recorded time period. The time interval (median [IQR]) of DP recurrence for the patients in AF after ablation (7 patients) decreased from 21.1 s [11.8 49.7s] to 15.7 s [6.5 18.2 s]. The DF inside the DPs presented lower temporal standard deviation (0.18±0.06 Hz vs. 0.29±0.12 Hz, $p<0.05$) and higher OI (0.35±0.03 vs. 0.31±0.04, $p<0.05$). The atrial regions with the highest proportion of HDF region were the septum and the left upper pulmonary vein.
Conclusion: Multiple recurrent spatiotemporal HDF patterns exist during persAF. The proposed method can identify and quantify the spatiotemporal repetition of the HDFs, where the high recurrences of DP may suggest a more organised rhythm. DPs presented a more consistent DF and higher organisation compared with non-DPs, suggesting that DF with higher OI might be more likely to recur. Recurring patterns offer a more comprehensive dynamic insight of persAF behaviour, and ablation targeting such regions may be beneficial.

Contribution to the field

Dear Editorial Board of Frontiers in Physiology, Cardiac Electrophysiology, Please find enclosed our manuscript entitled "Automatic Extraction of Recurrent Patterns of High Dominant Frequency Mapping during Human Persistent Atrial Fibrillation" for consideration of publication in the Frontiers in Physiology, Cardiac Electrophysiology. We certify that none of the paper's contents

have been previously published and the paper is not under review with any other journal. All co-authors have read and approved the manuscript. Radiofrequency ablation targeting atrial regions with high dominant frequency (DF) resulted in suboptimal outcomes for persistent atrial fibrillation (persAF) treatment. However, only sequential mapping approaches were used in previous studies with the assumption of the temporal stability of DF. Our previous work has showed that DF is spatiotemporally unstable, but some patterns may recur in time. In this work, we have developed an automated tool to investigate such recurrent behaviours and their spatiotemporal regularity, which might provide further details of the underlying mechanisms that sustain the arrhythmia. We believe that our findings would be of interest to the readers of the Frontiers in Physiology, Cardiac Electrophysiology because the proposed tool may offer a more comprehensive overview of the persAF dynamic behaviour and the impact of ablation. Yours sincerely, Dr Xin Li

Funding statement

This work was supported by the NIHR Leicester Biomedical Research Centre, UK. Dr. Li received research grants from Medical Research Council UK (MRC DPFS ref: MR/S037306/1). Dr. Almeida received research grants from the British Heart Foundation (BHF Project Grant no. PG/18/33/33780), BHF Research Accelerator Award funding and Fundação de Amparo à Pesquisa do Estado de São Paulo (FAPESP, Brazil, Grant N. 2017/00319-8). Professor Ng received funding from the British Heart Foundation (BHF Programme Grant, RG/17/3/32774).

Ethics statements

Studies involving animal subjects

Generated Statement: No animal studies are presented in this manuscript.

Studies involving human subjects

Generated Statement: The studies involving human participants were reviewed and approved by the local ethics committee at the University Hospitals of Leicester NHS Trust and local NHS research ethics committee. . The patients/participants provided their written informed consent to participate in this study.

Inclusion of identifiable human data

Generated Statement: No potentially identifiable human images or data is presented in this study.

Data availability statement

Generated Statement: The original contributions presented in the study are included in the article/supplementary material, further inquiries can be directed to the corresponding author/s.

Automatic Extraction of Recurrent Patterns of High Dominant Frequency Mapping during Human Persistent Atrial Fibrillation

Xin Li*[1,2], Gavin S Chu*[1], Tiago P Almeida[1,2], Frederique J Vanheusden[3], João Salinet[4], Nawshin Dastagir[5], Amar R Mistry[1], Zakariyya Vali[1,6], Bharat Sidhu[1], Peter J Stafford[6], Fernando S Schlindwein[2,6], G André Ng[1,6]

[1]Department of Cardiovascular Science, University of Leicester, UK;

[2]School of Engineering, University of Leicester, UK;

[3]School of Science & Technology, Nottingham Trent University, UK;

[4]Biomedical Engineering, Centre for Engineering, Modelling and Applied Social Sciences (CECS), Federal University of ABC, Brazil; [5]Auckland Bioengineering Institute, University of Auckland, New Zealand

[6]National Institute for Health Research Leicester Cardiovascular Biomedical Research Centre, Glenfield Hospital, UK

*** Correspondence:**

Dr. Xin Li,
Department of Cardiovascular Sciences/School of Engineering
University of Leicester, LE1 7RH, UK
Tel: +44 (0) 116 229 7380
Email: xl251@leicester.ac.uk

* These authors contributed equally to the manuscript

Keywords: Atrial fibrillation, catheter ablation, non-contact mapping, atrial electrograms, dominant frequency, recurrent patterns, spatiotemporal patterns

Abstract

Purpose: Identifying targets for catheter ablation remains challenging in persistent atrial fibrillation (persAF). The dominant frequency (DF) of atrial electrograms during atrial fibrillation (AF) is believed to primarily reflect local activation. Highest DF (HDF) might be responsible for the initiation and perpetuation of persAF. However, the spatiotemporal behaviour of DF remains not fully understood. Some DFs during persAF were shown to lack spatiotemporal stability, while others exhibit recurrent behaviour. We sought to develop a tool to automatically detect recurrent DF patterns in persAF patients.
Methods: Non-contact mapping of the left atrium (LA) was performed in 10 patients undergoing persAF HDF ablation. 2048 virtual electrograms (vEGMs, EnSite Array, Abbott Laboratories, USA) were collected for up to 5 min before and after ablation. Frequency spectrum was estimated using fast Fourier transform and DF was identified as the peak between 4-10 Hz and organization index (OI) was calculated. The HDF maps were identified per 4-second window and an automated pattern recognition algorithm was used to find recurring HDF spatial patterns. Dominant patterns (DPs) were defined as the HDF pattern with the highest recurrence.
Results: DPs were found in all patients. Patients in atrial flutter after ablation had a single DP over the recorded time period. The time interval (median [IQR]) of DP recurrence for the patients in AF after ablation (7 patients) decreased from 21.1 s [11.8 49.7s] to 15.7 s [6.5 18.2 s]. The DF inside the DPs presented lower temporal standard deviation (0.18±0.06 Hz *vs.* 0.29±0.12 Hz, $p<0.05$) and higher OI (0.35±0.03 *vs.* 0.31±0.04, $p<0.05$). The atrial regions with the highest proportion of HDF region were the septum and the left upper pulmonary vein.
Conclusion: Multiple recurrent spatiotemporal HDF patterns exist during persAF. The proposed method can identify and quantify the spatiotemporal repetition of the HDFs, where the high recurrences of DP may suggest a more organised rhythm. DPs presented a more consistent DF and higher organisation compared with non-DPs, suggesting that DF with higher OI might be more likely to recur. Recurring patterns offer a more comprehensive dynamic insight of persAF behaviour, and ablation targeting such regions may be beneficial.

1 Introduction

Atrial fibrillation (AF) is the most common cardiac arrhythmia in clinical practice, affecting 1-2% of the population worldwide (1). AF increases the risk of stroke five-fold and is associated with increased heart failure, mortality and higher healthcare utilisation costs (1). Although catheter ablation is an effective therapy for paroxysmal AF (pAF) (2, 3), the identification of areas for successful ablation in patients with persistent AF (persAF) remains a challenge due to the existence of complex arrhythmogenic mechanisms (1, 4, 5).

Previous studies have shown that sustained AF induces structural and electrical remodelling in atrial tissue (6). These regions can potentially host focal ectopic activity and re-entry circuits, resulting in rapid local activations (7), which are important in triggering and perpetuating atrial arrhythmias. Atrial electrograms (EGMs) acquired from such atrial substrate regions have short cycle length. Dominant frequency (DF) has been introduced as a measure of the local activations from EGMs collected during AF (Figure 1) (8). High DF (HDF) has been shown to represent atrial regions with rapid electrical activation rates, which might be related to remodelled atrial substrate and, therefore, could be targets for ablation (9).

Clinical studies with DF-guided ablation reported suboptimal results. A small clinical study that first demonstrated combining pulmonary vein isolation (PVI) with ablation of maximum DF sites achieved a success rate of 56% in persAF patients (10). Later, a prospective randomized clinical trial of 232 patients with paroxysmal and persistent AF reported no improvement in ablation outcomes with a DF-guided approach compared with PVI alone (11). However, only sequential mapping approaches were used in those studies, with the implicit assumption of temporal stability of DF.

We have previously found that DF is spatiotemporally unstable when using high-density non-contact mapping (NCM) in the left atrium (LA) (12). This finding questions the appropriateness of using sequential data collection in DF mapping. More interestingly, our recent work suggested that some HDFs might present recurrent behaviour, in which HDF activity reappears in the same atrial region in different time instants (13). Therefore, we hypothesise that atrial regions with recurrent HDF activity might provide further details of the underlying mechanisms that sustain AF. The main objective of this study is to develop an automated tool to investigate the recurrent behaviour of HDF maps and its spatiotemporal repetition. Through detailed investigation of recurrent HDF maps, the underlying spatiotemporal periodicity of atrial activity could be unveiled and may offer a more comprehensive insight of dynamic behaviour in underlying persAF and the impact of ablation.

2 Methods

2.1 Electrophysiological study

The present USURP-AF (Understanding the electrophysiological SUbstRate of Persistent Atrial Fibrillation) study was approved by the local ethics committee at the University Hospitals of Leicester NHS Trust and local NHS research ethics committee. Ten patients undergoing catheter ablation for persAF for the first time were recruited. Details of the patients' baseline characteristics are presented in **Table 1**.

Prior to the ablation, all drugs except amiodarone were stopped for at least 4 half-lives. During the procedure, bilateral femoral venous access was obtained under fluoroscopic guidance, and a quadripolar catheter and a deflectable decapolar catheter were placed at the His position and Coronary Sinus (CS), respectively. Trans-septal puncture was performed to gain access to the left atrium (LA). A noncontact multi-electrode array (MEA) catheter (EnSite Velocity, Abbott Laboratories, USA) and a conventional deflectable mapping catheter were deployed in the LA. Anticoagulant drugs were administered to maintain an activated clotting time > 300 s. A high-resolution 3D geometry of the LA

was created using EnSite Velocity electro-anatomical mapping system (Abbott Laboratories, **Figure 1**) and anatomical locations were annotated. Virtual EGMs (vEGMs) were recorded for up to five minutes. Baseline recording was collected for up to 5 minutes, from which a 30 s segment was exported and analysed during the procedure to obtain the HDF sites in the LA using an in-house computer application (14). High DF regions in the LA were identified as previously described (13). The clusters of centres of HDF sites were targeted for ablation (14) (**Figure S12, Supplementary Material)**. Following DF-guided ablation, a post-ablation recording was collected for up to 5 minutes, following which pulmonary vein isolation (PVI) was carried out with the circular, multipolar PVAC catheter (Medtronic Inc.). Four out of ten patients had AF termination (3 atrial flutter (AFL, 1 sinus rhythm) by HDF ablation prior to PVI (15). There were no adverse events in any of our ten patients.

2.2 Data acquisition and signal processing

Intracardiac signals were collected using the non-contact MEA catheter as described above. The vEGMs (2048 channels) were sampled at 2034.5 Hz and exported with the filter setting of 1 Hz to 150 Hz. The data was analysed offline using MATLAB R2013a (Mathworks, USA). The vEGMs were resampled to 512 Hz using cubic spline interpolation method to reduce processing time while maintaining a relatively high sampling rate for the frequency analysis. As illustrated in **Figure 1**, ventricular far-field activity was removed from the recorded vEGMs using a QRST subtraction technique previously described (16). The vEGMs were then divided into 4 s window segments with a 50% overlap. For each segment, spectral analysis was performed using fast Fourier transform (FFT). A Hamming window was applied to the atrial vEGMs to reduce leakage. Zero padding was used to improve the DF identification with a resulting frequency step of 0.05 Hz. DF was defined as the peak in the power spectrum within the physiological range of 4-10 Hz (13).

2.3 HDF Pattern Extraction

HDFs were defined as atrial nodes with DF values equal to or greater than the top 10th percentile DF values across the LA surface for each time window. Binary HDF maps were generated for all windows, where HDF regions were marked as 'ones' and low DF (LDF) regions were marked as zeros 'zeros' (**Figure 1**). The vEGMs of 2048 virtual electrodes were mapped onto a 64×32 2D rectangular grid, as previously described (17). The 2D binary HDF maps (graphic pattern) were used as the input of the pattern extraction algorithm based on 2D correlation (18), to find the reappearing HDF maps in time and cluster the maps into patterns.

A 2D Pearson's correlation coefficient (CORR) (Equation 1) was used as a measurement of similarity between the HDF maps at different time windows. Here, A, B represent the 2D HDF maps; $\bar{A}, \bar{B}$ their average values; and i and j are the row and column of the images.

$$CC = \frac{\sum\sum\left(A_{ij} - \bar{A}\right)\left(B_{ij} - \bar{B}\right)}{\sqrt{\left(\sum\sum\left(A_{ij} - \bar{A}\right)^2\right)\left(\sum\sum\left(B_{ij} - \bar{B}\right)^2\right)}} \qquad \text{Equation 1}$$

Figure 2A contains the flowchart of HDF pattern extraction algorithm, in which all the generated 2D HDF maps are referred to as the 'data pool' and a single HDF map is referred to as an 'element'. Briefly, the key steps of the algorithm can be explained as:

- Step 1: Compute the CORR of first element of the data pool with the rest, set the elements with CORR greater than a threshold and the current element (CE) defined as current pattern (CP).

- Step 2: Calculate the CORR of the other elements (if there are any) in CP with the elements in the data pool and add the elements greater than the threshold to CP. Remove the CP maps from the data pool, repeat this until there are no elements joining the CP at the last element.
- Step 3: Consider as a pattern if more than one element is found and move on to the next pattern.
- Step 4: Repeat steps 1, 2 and 3 until there are no more elements in the data pool. Sort the patterns by number of elements.

The CORR threshold was set as 0.6 for the analysis. Effects of the CORR threshold of the pattern extraction algorithm are discussed in the **Supplementary Material.** Please note the algorithm generates consistent patterns with arbitrary choice of first element of the data pool, as pattern elements will finally converge when no elements outside the pattern can generate CORR greater than threshold with any element in the current pattern.

2.4 Temporal Pattern Analysis

The pattern extraction algorithm was applied to the HDF maps of the ten patients before and after DF-guided ablation. **Figure 2B** illustrates one example of all the patterns for one patient. In order to investigate the recurrence of events, the dominant pattern (DP) was defined as the HDF pattern with the highest recurrence (Pattern 1).

2.5 Feature Analysis of the Dominant Pattern

The mean and standard deviation of the DF, and the organization index (OI) of the HDF regions of each map were calculated. OI is defined as the area under the curve of DF peak divided by the area under the curve of the entire power spectrum (19, 20). The average and standard deviation of DF and OI of the DP windows and the non-DP windows were compared.

To study the behaviour of secondary DPs, the mean and standard deviation of the DF, and the organization index (OI) of the HDF regions of each map were calculated. The DF and OI in the HDF regions of the secondary DPs (i.e., 2nd dominant, and 3rd dominant patterns) were compared. The average and standard deviation of DF and OI of the DP windows, secondary DPs and the non-DP windows were compared.

2.6 Regional Analysis

The LA geometries of the ten patients were manually segmented by an experienced clinician into 12 regions – Mitral valve (MV); Left upper pulmonary vein (LUPV); Left lower PV (LLPV); Right upper PV (RUPV); Right lower PV (RLPV); Roof; Posterior (Pos); Anterior (ant); LA appendage (LAA); MV isthmus (MVI); Septum (sept); Floor. The segmentation was manually performed on the EnSite Velocity System by creating virtual 3D surface lesion points to form closed loop boundary points for each anatomical region. The numbering of 3D locations was recorded and saved in Microsoft Excel format. An automated MATLAB software was developed to read the data and the corresponding 3D coordinates (lesion files) of the boundary lesion points. For each set of the boundary lesion points, a closed 3D polygonal mesh was created using Delaunay triangulation. Vectors were created connecting the centre point of the LA mesh and surface nodes locations, and regional labels were estimated according to the intersection between the vectors and any of the triangular faces of the 3D polygon mesh. Thus, surface nodes of the triangular mesh within boundary points were detected for all regions, and all vEGMs were assigned to anatomical labels. The DP HDF occurrence at all anatomic regions were counted.

2.7 Statistical Analysis

Wilcoxon matched-pairs signed rank tests were performed to compare the mean time intervals before and after ablation. The average and standard deviation of DF and OI of the DP windows and the non-DP windows were also compared using Wilcoxon matched-pairs signed rank tests. DF and OI of the DP, secondary DPs and non-pattern windows were compared with unpaired ordinary one-way ANOVA, and each two classes were compared with unpaired t tests. The average and standard deviation of DF and OI of DP, secondary DPs and non-pattern windows were compared with paired one-way ANOVA, and each two classes were compared with paired t tests. One-way ANOVA was used to compare the regions hosting DP. A P-value below 0.05 was considered significant in all statistical tests.

3 Results

A total of 2793 DF maps were analysed, in a total of 2983.5 seconds before and 2664.5 seconds after DF-guided ablation. Recurrent patterns were found on all ten patients before and after ablation using the proposed algorithm.

3.1 Recurrence of HDF patterns

The time windows in which the DPs occurred were annotated before and after ablation for all the patients in order to investigate their periodic behaviours. An example of the DP recurrences and their atrial locations for one of the patients is illustrated in **Figure 3A**. The temporal behaviour of the DPs for each patient is shown in **Figure 3B**. The time instants in which the DPs occurred are marked in black. Both the percentage of duration of the DP windows and the mean intervals between the time windows hosting DPs have been measured in order to assess the incidence of DP recurrences (Table 2).

HDF-guided ablation therapy prior PVI increased the DPs occurrence in 7 out of 10 patients, suggesting increased AF organisation following ablation, as illustrated in **Figure 3B**. In general, the time interval (median [IQR]) of DP recurrence for all patients decreased from 16.8 s [11.5-32.4 s] to 6.5 s [3.3-16.0 s] after ablation (p=0.13). Patients 4, 5 and 10 converted to atrial flutter following ablation. The post-ablation DP accounted for 68.1% for patient 4, 94.8% for patient 5 and 93.6% for patient 10 of the total recorded windows, which corroborates the robustness of the method in capturing underlying recurrent DF patterns (**Table 2**). The time interval of DP recurrence for the patients remaining in AF (excluding patients 4, 5 and 10) after ablation decreased from 21.1 s [11.8-49.7 s] to 15.7s [6.5-18.2 s] (p=0.29).

Please note, as mentioned in Section 2.3, the CORR threshold was set as 0.6 for the analysis to allow a sufficient number of recurrences for all patients (see **Figure S11** in the **Supplementary Material**). This choice may have some effects on the above results of recurrences.

3.2 DP features

The DF and OI in the HDF regions for all the maps were calculated. **Figure 4A** illustrates the recurring HDF maps and the time window occurrences of the DP. The average frequency in HDF regions inside the DPs was 6.25±0.73 Hz, and 6.26±0.70 Hz in non-DPs (p=0.92; **Figure 4Bi**). However, the standard deviation of mean DF in HDF regions in the DPs was significant lower when compared with that outside the DPs (0.18 ± 0.06 Hz *vs.* 0.29 ± 0.12 Hz, p<0.05; **Figure 4Bii**). Additionally, the OI was significantly higher in the DP regions compared to non-DP regions (0.35 ± 0.03 *vs.* 0.31 ± 0.04, p<0.05; **Figure 4Biii**).

3.3 Regional difference of DP occurrence

As illustrated in **Figure 5A**, the anatomic regions were segmented and HDF visits from DPs for each region were calculated. The proportion of HDF regions in DP on each anatomic region are summarised in **Figure 5B**. The distributions varied among regions ($p<0.01$). The regions hosting DPs most often were the septum and the LUPV (**Figure 5C**).

3.4 Secondary DP features

As illustrated in **Figure 6A**, the DFs inside the HDF regions of the DP, 2nd DP, 3rd DP windows and non-DP were significantly different (5.65±0.70 Hz *vs.* 5.59±0.85 Hz *vs.* 5.54±0.81 Hz *vs.* 6.18±0.88 Hz, $p<0.0001$). DFs were shown to reduce with the decreased hierarchy of patterns (i.e., from 1st DP to 3rd DP, $p<0.0001$), but were all significantly smaller than the non-DP windows ($p<0.0001$). **Figure 6B** demonstrates that OIs inside the HDF regions were significantly different (DP: 0.37±0.13; 2nd DP: 0.36±0.14; 3rd DP: 0.35±0.14; and non-DP: 0.32±0.13, $p<0.0001$). OIs directly decreased according to the decreasing order of dominance of the patterns (i.e., from 1st DP to 3rd DP, and then to non-DP windows, $p<0.0001$). In **Figure 6C,** the standard deviation of mean DF in HDF regions across pattern windows were 0.125±0.065 Hz for DP, 0.164±0.135 Hz for 2nd DP; and 0.093±0.066 Hz for 3rd DP ($p=0.1774$ for DP *vs.* 2nd DP; $p=0.3558$ for DP *vs.* 3rd DP; $p=0.2135$ for 2nd DP *vs.* 3rd DP), but they were significantly lower when compared with the non-DP individually (0.240±0.148 Hz; $p=0.0033$ for DP *vs.* non-DP; $p=0.0016$ for 2nd DP *vs.* non-DP; $p=0.0274$ for 3rd DP *vs.* non-DP). As illustrated in **Figure 6D**, multiple patterns existed in all patients and a higher portion of DPs and secondary DPs were observed after ablation in most of the patients. Details of all the recurrent patterns from all patients can be found in the **Supplementary materials**.

4 Discussion

In this study, we developed an automated tool that characterises the recurrent behaviour of HDF maps and its spatiotemporal repetition. We are the first to show that different patterns of DF consistently reappear in the LA during human persAF, providing valuable insights regarding the underlying spatiotemporal behaviour and complexity of this arrhythmia. Although persAF is characterized by turbulent activations, the recurrence of DF patterns could indicate AF drivers which may have been anchored in the substrate. With detailed investigation of recurrent HDF maps, the underlying spatiotemporal periodicity of atrial activity could be unveiled and may offer a more comprehensive insight of the dynamic behaviour of persAF. We have also shown that there exist recurrent spatial patterns at different levels of periodicity and present summaries of the types of spatial patterns that may be more likely to recur. Detailed investigations of these recurrent spatial patterns could further help to define the potential targets for ablation.

4.1 HDF Pattern Recurrences

Previous studies have shown that the DFs of individual vEGMs are temporally unstable when mapped with NCM, where a recurrent behaviour in HDF reappearance was noticed in the LA, sometimes within 10 seconds (13). In the present study, multiple recurrent activities were found for most of the patients using the proposed pattern extraction technique on NCM signals. This finding reinforces the idea that persAF is not entirely random, and that instead, various degrees of spatiotemporal organization may co-exist (21, 22). Despite the evident complexity of AF sustained by the meandering of multiple wavelets (23), wave collision (24), or breakthrough activations (25), some atrial regions present remarkable recurrent activation with a certain degree of organization. These activities could therefore be explained by ectopic activities (3, 26) and local re-entries (27). Additionally, one single DP was

found in patients whose AF converted to atrial flutter following HDF-guided ablation. This was expected since atrial flutter is an organised arrhythmia compared to AF (28). Atrial flutter is usually sustained by one macro re-entrant circuit and, therefore, the organized spatiotemporal behaviour – i.e., faster and with more reappearances – of the DPs correlates with the higher level of regularity of atrial flutter. This finding could also support and help validate the potential use of the proposed method in describing spatiotemporal regularization from AF to more organised tachyarrhythmia. In addition, an overall increase of DP recurrence was found after ablation, suggesting catheter ablation in this cohort of patients may have increased the spatiotemporal regularization and transformed a complex persAF rhythm to a less complex and more organised tachyarrhythmia. Nevertheless, patients 4 and 5 had lowest DPs occurrences prior to ablation responded well to ablation, which may suggest that a less organised rhythm could still be converted with appropriate ablation.

4.2 DP Features – what frequency features are more likely to recur?

To investigate whether specific EGM features could predict HDF recurrence, binary HDF maps were set as input of the algorithm, so that the system was blind to the DF values of each HDF map. In other words, only the location and shape of the HDF maps were taken in consideration with regard to studying the recurrence behaviour. Although the reappearing HDF maps were not dependent on the DF value that defined the HDF region, lower standard deviations of the mean DF within the DPs were found, which suggests that higher temporal consistency of the detected pattern over the non-pattern maps (i.e., when a map is recurrent in time, there is a high chance that the DF would be more similar than other non-recurring maps). OI has been proposed as a method to measure the 'dominance' of the DF in atrial sites (19, 20). Our findings show the OI of the recurrent HDF maps to be higher in DP than in non-DP regions. HDF maps with higher OI being more likely to reappear further supports the hypothesis of the existence of underlying periodic atrial activity during AF. This may suggest that more organised periodic atrial activity may be more likely to drive the rhythm and might have a higher chance of showing a recurring spatial pattern.

In the analysis of secondary patterns, we found that the recurrent patterns did not necessarily have the highest frequency across all time windows. This could suggest that the higher non-recurrent frequency could be a passive phenomenon (wave collisions) (24, 25) and an unwanted harmonic frequency (multiples of the fundamental frequency) (29). This was also supported by the results that spectral organisation decreased from the most recurring pattern to less recurrent and dropped to a minimum at non-recurring patterns (**Figure 6B**). There was also a decrease in DFs from the most recurrent pattern to the least recurrent pattern, suggesting that patterns with high organisation and relative high frequency could be more likely to recur in time with similar location and graphic pattern.

4.3 Regional Pattern Distribution

The distribution of the recurrent DP areas varied among atrial regions for all patients. Our results suggest that the LUPVs and the septum are more likely to host DPs. Considering that PVs have been shown important in the initiation and maintenance of AF, and that usually maximum DF sites can be found near the PVs (9, 10, 30), it could be expected that the PVs might also be preferred sites to host DPs. Additionally, our findings suggest that the septum is one of the regions prone to host recurrent behaviours, which is in agreement with previous studies that have shown the septum as one of the critical sites for AF termination during ablation (31-37).

4.4 'Recurrent patterns' in AF

AF is a complex rhythm and often shows complex propagation patterns. This poses significant challenges to narrow down the potential driver sites using atrial signals often captured: 1) during single

cycles of activation or short signal lengths (i.e., 2.5 seconds); 2) from single or localised atrial site(s); and 3) sequentially. Therefore, the search for 'recurrent patterns' in AF is not a new concept but unveiling the underlying driving mechanisms from their recurrent behaviours is only possible with longer recordings from multiple atrial sites. Ng J. *et al.* proposed using 'recurrence plots' of selected activations from individual EGMs in the time domain, showing checkerboard patterns of alternating high and low cross-correlation values indicating periodic recurrent patterns in the morphologies of atrial activations (38). Their approach was based on the morphologies of the EGMs which are useful for identifying recurring local activations (waves propagated from similar directions) but may not guarantee a recurrent graphic pattern with larger atrial regions involved. Simultaneous multipolar recordings were used in more recent studies, including phase mapping (39-42). Multi-site phase mapping was used to map the wave propagations, with complex patterns observed. However, stable 'rotors' or phase singularities were rarely seen (17, 43, 44) and, therefore, statistical approaches were usually employed, such as the repetitive activation patterns (RAPs) (45), and PS density (histogram) maps (17), both able to quantify the recurrent behaviours of the core of the 'rotor' visiting the same atrial location over time.

It is still debatable whether these localised rotational behaviours are true representatives of AF drivers or caused by conduction delay or blocks (44, 46). A recently reported approach to explore recurrent patterns was the use of the CARTOFINDER system (Biosense Webster, USA) (47). It analyses 30 seconds of unipolar signals obtained from the 64 poles of the basket catheters or the regional 20-pole PENTARAY catheter (47). Recurrent rotational and focal activities can be identified from multi-site simultaneous contact EGMs. However, like other activation-based methods, the accuracy of this method is highly dependent on the robustness and accuracy of the annotation algorithm used to analyse intracardiac signals, which could be a common challenge for most time domain analyses (48). Nevertheless, these are important studies and will be of great interest for testing the common hypothesis that atrial sites with rapid activation of highly repetitive patterns may be critical to sustaining AF. NCM has become less favoured for mapping AF due to the low 'morphology accuracy' for sites with electrode-to-surface distance greater than 4 cm (49-52). However, NCM could potentially provide ideal data for recurrent activity analysis, especially in the frequency domain (53). Using NCM data, the proposed method has demonstrated the ability to find recurrent spatial patterns showing interesting multi-level organisation and recurrent behaviours with great potential to unveil true driving mechanisms, with the advantages of using long signal duration from a whole-chamber coverage, and without the limitation of requiring time-domain annotations.

5 Limitations

This study involves a relatively small number of patients to explore the recurrent HDF patterns using high-density NCM during persAF. Nevertheless, a large number of EGMs with long signal lengths were investigated. The method proposed in the paper, like others, is reliant on predefined parameters. Further investigation on optimising the parameters should be carried out in future work. The recurrent HDF regions found by the algorithms demonstrated organised behaviours and might be good candidates for ablation, however, this should be throughout validated and confirmed in a clinical trial.

6 Conclusions

In this study, we have developed and introduced a new tool to investigate the spatiotemporal behaviour of HDF in patients with persAF. Our results suggest that multiple recurrent spatiotemporal HDF patterns co-exist during persAF, with different frequencies and levels of spectral organisation. The high recurrences of DP suggest a more organised rhythm. The pattern extraction algorithm can summarize the underlying non-random periodic atrial frequency activity, identifying and quantifying

the spatiotemporal recurrence of the HDFs. We also found that electrograms with high organisation and relative high frequency recur in time, producing similar graphic patterns. The investigation of recurrent HDF regions at different levels offer a more comprehensive dynamic insight of persAF behaviour, and such regions might be good candidates for ablation.

7 Acknowledgements

Dr. Schlindwein is grateful for a study leave by the University of Leicester in 2019-20.

8 Conflicts of interest

Professor Ng has received a research fellowship from St. Jude Medical (now Abbott) and speaker fees and honoraria from Biosense Webster. All other authors have reported that they have no relationships relevant to the contents of this paper to disclose.

9 Author contributions

XL: concept/design study, data analysis/interpretation of results, drafting manuscript, critical revision of manuscript, statistics, and 'off-line' data collection; GSC: concept/design study, data analysis/interpretation of results, drafting manuscript, critical revision of manuscript, statistics, and 'off-line' data collection; TPA: data analysis/interpretation of results, drafting manuscript, critical revision of manuscript, statistics; FJV: data analysis/interpretation of results, critical revision of manuscript, statistics; JS: data analysis/interpretation of results, critical revision of manuscript; ND: data analysis/interpretation of results, critical revision of manuscript, statistics; ARM: data analysis/interpretation of results, critical revision of manuscript; ZV: data analysis/interpretation of results, critical revision of manuscript, statistics; BS: data analysis/interpretation of results, critical revision of manuscript, statistics; PJS: EP study, data collection, interpretation of results, critical revision of manuscript; FSS: Concept/design study, data analysis/interpretation of results, critical revision of manuscript; GAN: EP studies and ablation procedures, concept/design study, interpretation of results, critical revision of manuscript.

10 Funding

This work was supported by the NIHR Leicester Biomedical Research Centre, UK. Dr. Li received research grants from Medical Research Council UK (MRC DPFS ref: MR/S037306/1). Dr. Almeida received research grants from the British Heart Foundation (BHF Project Grant no. PG/18/33/33780), BHF Research Accelerator Award funding and Fundação de Amparo à Pesquisa do Estado de São Paulo (FAPESP, Brazil, Grant N. 2017/00319-8). Professor Ng received funding from the British Heart Foundation (BHF Programme Grant, RG/17/3/32774).

11 References

1. Nattel S. New ideas about atrial fibrillation 50 years on. Nature. 2002;415(6868):219-26.

2. Fichtner S, Sparn K, Reents T, Ammar S, Semmler V, Dillier R, et al. Recurrence of paroxysmal atrial fibrillation after pulmonary vein isolation: is repeat pulmonary vein isolation enough? A prospective, randomized trial. Europace. 2015;17(9):1371-5.

3. Haissaguerre M, Jais P, Shah DC, Takahashi A, Hocini M, Quiniou G, et al. Spontaneous initiation of atrial fibrillation by ectopic beats originating in the pulmonary veins. New Engl J Med. 1998;339(10):659-66.

4. Jalife J, Berenfeld O, Mansour M. Mother rotors and fibrillatory conduction: a mechanism of atrial fibrillation. Cardiovasc Res. 2002;54(2):204-16.

5. Nattel S. Atrial electrophysiology and mechanisms of atrial fibrillation. J Cardiovasc Pharmacol Ther. 2003;8 Suppl 1(1 suppl):S5-11.

6. Goette A, Honeycutt C, Langberg JJ. Electrical remodeling in atrial fibrillation. Time course and mechanisms. Circulation. 1996;94(11):2968-74.

7. Ashihara T, Haraguchi R, Nakazawa K, Namba T, Ikeda T, Nakazawa Y, et al. The role of fibroblasts in complex fractionated electrograms during persistent/permanent atrial fibrillation: implications for electrogram-based catheter ablation. Circ Res. 2012;110(2):275-84.

8. Mansour M, Mandapati R, Berenfeld O, Chen J, Samie FH, Jalife J. Left-to-right gradient of atrial frequencies during acute atrial fibrillation in the isolated sheep heart. Circulation. 2001;103(21):2631-6.

9. Sanders P, Berenfeld O, Hocini M, Jais P, Vaidyanathan R, Hsu LF, et al. Spectral analysis identifies sites of high-frequency activity maintaining atrial fibrillation in humans. Circulation. 2005;112(6):789-97.

10. Atienza F, Almendral J, Jalife J, Zlochiver S, Ploutz-Snyder R, Torrecilla EG, et al. Real-time dominant frequency mapping and ablation of dominant frequency sites in atrial fibrillation with left-to-right frequency gradients predicts long-term maintenance of sinus rhythm. Heart Rhythm. 2009;6(1):33-40.

11. Panikker S, Jarman JW, Virmani R, Kutys R, Haldar S, Lim E, et al. Left Atrial Appendage Electrical Isolation and Concomitant Device Occlusion to Treat Persistent Atrial Fibrillation: A First-in-Human Safety, Feasibility, and Efficacy Study. Circ Arrhythm Electrophysiol. 2016;9(7).

12. Jarman JW, Wong T, Kojodjojo P, Spohr H, Davies JE, Roughton M, et al. Spatiotemporal behavior of high dominant frequency during paroxysmal and persistent atrial fibrillation in the human left atrium. Circ Arrhythm Electrophysiol. 2012;5(4):650-8.

13. Salinet JL, Tuan JH, Sandilands AJ, Stafford PJ, Schlindwein FS, Ng GA. Distinctive patterns of dominant frequency trajectory behavior in drug-refractory persistent atrial fibrillation: preliminary characterization of spatiotemporal instability. J Cardiovasc Electrophysiol. 2014;25(4):371-9.

14. Li X, Salinet JL, Almeida TP, Vanheusden FJ, Chu GS, Ng GA, et al. An interactive platform to guide catheter ablation in human persistent atrial fibrillation using dominant frequency, organization and phase mapping. Comput Methods Programs Biomed. 2017;141:83-92.

15. Chubb H, Chu GS, Qureshi NA, Gamble JHP, Sohaib SMA, Taylor RJ, et al. Young Investigators Competition1Left ventricular lead position, mechanical activation and myocardial scar in relation to the clinical outcome of cardiac resynchronisation therapy: the role of feature-tracking and contrast-enhanced cardiovascular magnetic resonance2Does the haemodynamic improvement of biventricular pacing truly arise from cardiac resynchronisation? quantifying the contribution of av and vv adjustment3Differential relationship of electrical delay with endocardial and epicardial left ventricular leads for cardiac resynchronisation therapy4Characterisation of the persistent af substrate through the assessment of electrophysiologic parameters in the organised vs. disorganised rhythm5Targeting cyclical highest dominant frequency in the ablation of persistent atrial

fibrillation6Feasibility of fully mr-guided ablation with active tracking: from pre-clinical to clinical application. Europace. 2016;17(suppl 5):v1-v2.

16. Salinet JL, Jr., Madeiro JP, Cortez PC, Stafford PJ, Ng GA, Schlindwein FS. Analysis of QRS-T subtraction in unipolar atrial fibrillation electrograms. Med Biol Eng Comput. 2013;51(12):1381-91.

17. Li X, Almeida TP, Dastagir N, Guillem MS, Salinet J, Chu GS, et al. Standardizing Single-Frame Phase Singularity Identification Algorithms and Parameters in Phase Mapping During Human Atrial Fibrillation. Front Physiol. 2020;11:869.

18. Li X, Chu GS, Almeida TP, Vanheusden FJ, Dastagir N, Salinet JL, et al., editors. Investigation on recurrent high dominant frequency spatiotemporal patterns during persistent atrial fibrillation. Computing in Cardiology Conference (CinC), 2015; 2015 6-9 Sept. 2015.

19. Everett THt, Kok LC, Vaughn RH, Moorman JR, Haines DE. Frequency domain algorithm for quantifying atrial fibrillation organization to increase defibrillation efficacy. IEEE Trans Biomed Eng. 2001;48(9):969-78.

20. Jarman JWE, Wong T, Kojodjojo P, Spohr H, Davies JER, Roughton M, et al. Organizational index mapping to identify focal sources during persistent atrial fibrillation. J Cardiovasc Electrophysiol. 2014;25(4):355-63.

21. Gerstenfeld EP, Sahakian AV, Swiryn S. Evidence for transient linking of atrial excitation during atrial fibrillation in humans. Circulation. 1992;86(2):375-82.

22. Botteron GW, Smith JM. Quantitative assessment of the spatial organization of atrial fibrillation in the intact human heart. Circulation. 1996;93(3):513-8.

23. Wijffels MCEF, Kirchhof CJHJ, Dorland R, Allessie MA. Atrial-Fibrillation Begets Atrial-Fibrillation - a Study in Awake Chronically Instrumented Goats. Circulation. 1995;92(7):1954-68.

24. Allessie MA, Kirchhof CJ, Konings KT. Unravelling the electrical mysteries of atrial fibrillation. Eur Heart J. 1996;17 Suppl C:2-9.

25. Gray RA, Pertsov AM, Jalife J. Incomplete reentry and epicardial breakthrough patterns during atrial fibrillation in the sheep heart. Circulation. 1996;94(10):2649-61.

26. Chen SA, Hsieh MH, Tai CT, Tsai CF, Prakash VS, Yu WC, et al. Initiation of atrial fibrillation by ectopic beats originating from the pulmonary veins: electrophysiological characteristics, pharmacological responses, and effects of radiofrequency ablation. Circulation. 1999;100(18):1879-86.

27. Moe GK, Rheinboldt WC, Abildskov JA. A Computer Model of Atrial Fibrillation. Am Heart J. 1964;67:200-20.

28. Winter JB, Crijns HJ. Atrial flutter and atrial fibrillation: two sides of a coin or one coin? J Cardiovasc Electrophysiol. 2000;11(8):859-60.

29. Traykov VB, Pap R, Saghy L. Frequency domain mapping of atrial fibrillation - methodology, experimental data and clinical implications. Curr Cardiol Rev. 2012;8(3):231-8.

30. Oral H, Knight BP, Tada H, Ozaydin M, Chugh A, Hassan S, et al. Pulmonary vein isolation for paroxysmal and persistent atrial fibrillation. Circulation. 2002;105(9):1077-81.

31. Uldry L, Virag N, Lindemans F, Vesin JM, Kappenberger L. Atrial septal pacing for the termination of atrial fibrillation: study in a biophysical model of human atria. Europace. 2012;14 Suppl 5:v112-v20.

32. Schmitt C, Estner H, Hecher B, Luik A, Kolb C, Karch M, et al. Radiofrequency ablation of complex fractionated atrial electrograms (CFAE): preferential sites of acute termination and regularization in paroxysmal and persistent atrial fibrillation. J Cardiovasc Electrophysiol. 2007;18(10):1039-46.

33. Calo L, De Ruvo E, Sciarra L, Gricia R, Navone G, De Luca L, et al. Diagnostic accuracy of a new software for complex fractionated electrograms identification in patients with persistent and permanent atrial fibrillation. J Cardiovasc Electrophysiol. 2008;19(10):1024-30.

34. Porter M, Spear W, Akar JG, Helms R, Brysiewicz N, Santucci P, et al. Prospective study of atrial fibrillation termination during ablation guided by automated detection of fractionated electrograms. J Cardiovasc Electrophysiol. 2008;19(6):613-20.

35. Takahashi Y, O'Neill MD, Hocini M, Dubois R, Matsuo S, Knecht S, et al. Characterization of electrograms associated with termination of chronic atrial fibrillation by catheter ablation. J Am Coll Cardiol. 2008;51(10):1003-10.

36. Park JH, Pak HN, Kim SK, Jang JK, Choi JI, Lim HE, et al. Electrophysiologic characteristics of complex fractionated atrial electrograms in patients with atrial fibrillation. J Cardiovasc Electrophysiol. 2009;20(3):266-72.

37. Roux JF, Gojraty S, Bala R, Liu CF, Dixit S, Hutchinson MD, et al. Effect of pulmonary vein isolation on the distribution of complex fractionated electrograms in humans. Heart Rhythm. 2009;6(2):156-60.

38. Ng J, Gordon D, Passman RS, Knight BP, Arora R, Goldberger JJ. Electrogram morphology recurrence patterns during atrial fibrillation. Heart Rhythm. 2014;11(11):2027-34.

39. Narayan SM, Baykaner T, Clopton P, Schricker A, Lalani GG, Krummen DE, et al. Ablation of rotor and focal sources reduces late recurrence of atrial fibrillation compared with trigger ablation alone: extended follow-up of the CONFIRM trial (Conventional Ablation for Atrial Fibrillation With or Without Focal Impulse and Rotor Modulation). J Am Coll Cardiol. 2014;63(17):1761-8.

40. Narayan SM, Patel J, Mulpuru S, Krummen DE. Focal impulse and rotor modulation ablation of sustaining rotors abruptly terminates persistent atrial fibrillation to sinus rhythm with elimination on follow-up: a video case study. Heart Rhythm. 2012;9(9):1436-9.

41. Rodrigo M, Climent AM, Liberos A, Fernandez-Aviles F, Berenfeld O, Atienza F, et al. Technical Considerations on Phase Mapping for Identification of Atrial Reentrant Activity in Direct- and Inverse-Computed Electrograms. Circ Arrhythm Electrophysiol. 2017;10(9).

42. Umapathy K, Nair K, Masse S, Krishnan S, Rogers J, Nash MP, et al. Phase mapping of cardiac fibrillation. Circ Arrhythm Electrophysiol. 2010;3(1):105-14.

43. Salinet J, Schlindwein FS, Stafford P, Almeida TP, Li X, Vanheusden FJ, et al. Propagation of meandering rotors surrounded by areas of high dominant frequency in persistent atrial fibrillation. Heart Rhythm. 2017;14(9):1269-78.

44. Podziemski P, Zeemering S, Kuklik P, van Hunnik A, Maesen B, Maessen J, et al. Rotors Detected by Phase Analysis of Filtered, Epicardial Atrial Fibrillation Electrograms Colocalize With Regions of Conduction Block. Circ Arrhythm Electrophysiol. 2018;11(10):e005858.

45. Daoud EG, Zeidan Z, Hummel JD, Weiss R, Houmsse M, Augostini R, et al. Identification of Repetitive Activation Patterns Using Novel Computational Analysis of Multielectrode Recordings During Atrial Fibrillation and Flutter in Humans. JACC Clin Electrophysiol. 2017;3(3):207-16.

46. Li X, Sidhu B, Almeida TP, Ehnesh M, Mistry A, Vali Z, et al. P439Could regional electrogram desynchronization identified using mean phase coherence be potential ablation targets in persistent atrial fibrillation? EP Europace. 2020;22(Supplement_1).

47. Honarbakhsh S, Schilling RJ, Dhillon G, Ullah W, Keating E, Providencia R, et al. A Novel Mapping System for Panoramic Mapping of the Left Atrium: Application to Detect and Characterize Localized Sources Maintaining Atrial Fibrillation. JACC Clin Electrophysiol. 2018;4(1):124-34.

48. Tomassoni G. CARTOFINDER: Can it "Find" Rotors in Atrial Fibrillation? JACC Clin Electrophysiol. 2017;3(3):217-9.

49. Earley MJ, Abrams DJ, Sporton SC, Schilling RJ. Validation of the noncontact mapping system in the left atrium during permanent atrial fibrillation and sinus rhythm. J Am Coll Cardiol. 2006;48(3):485-91.

50. Schilling RJ, Peters NS, Davies W. Simultaneous endocardial mapping in the human left ventricle using a noncontact catheter - Comparison of contact and reconstructed electrograms during sinus rhythm. Circulation. 1998;98(9):887-98.

51. Thiagalingam A, Wallace EM, Boyd AC, Eipper VE, Campbell CR, Byth K, et al. Noncontact mapping of the left ventricle: insights from validation with transmural contact mapping. Pace. 2004;27(5):570-8.

52. Shi R, Parikh P, Chen Z, Angel N, Norman M, Hussain W, et al. Validation of Dipole Density Mapping During Atrial Fibrillation and Sinus Rhythm in Human Left Atrium. JACC Clin Electrophysiol. 2020;6(2):171-81.

53. Gojraty S, Lavi N, Valles E, Kim SJ, Michele J, Gerstenfeld EP. Dominant frequency mapping of atrial fibrillation: comparison of contact and noncontact approaches. J Cardiovasc Electrophysiol. 2009;20(9):997-1004.

12 Tables

Table 1: Clinical Characteristics of Patients

Patient Characteristics n=10 (male)			
Male (n)	10		
On amiodarone (n)	2		
	Median	Min	Max
Age (years)	57.8	36.1	76.4
Days in AF pre-procedure (days)	219	132	848
BMI	30.4	23.4	43.8
previous DCCVs	2	1	5
Days since last DCCV	487	224	1237
Procedure time (mins)	390	309	475
Fluoroscopy (mins)	77.2	51.4	98.5
Ablation (mins)	44.1	26.5	109.2
Ablation area (mm^2/ % of LA)	1368 (7.5)	627 (3.3)	2668 (13.6)

548
549 **Table 2:** The duration of the dominant pattern windows and the mean interval among subsequent
550 occurrences of patterns before and after ablation for all patients. AFL: atrial flutter; IQR: Interquartile
551 Range.

552

Patient	% DP Duration		Mean Interval (s)	
	Pre	Post	Pre	Post
1	1.4	9	132.00	20.31
2	17.4	4.9	11.23	37.14
3	43.2	12.7	4.38	15.68
4	11.5	68.1(AFL)	12.29	2.77
5	5.7	94.8 (AFL)	23.25	2.11
6	6.9	40.5	21.11	4.98
7	15.8	11.5	12.45	16.13
8	5.4	24.6	35.43	8.00
9	1.3	7.2	64.00	4.81
10	32.5	93.6 (AFL)	6.04	2.14
Median [IQR] All patients	9.2[5.4~17]	18.6[9.6~61.2]	16.8[11.5~32.4]	6.5[3.3~16.0]
Median [IQR] AF only	6.9[3.4~16.6]	11.5[8.1~18.7]	21.1[11.8~49.7]	15.7[6.5~18.2]

553

554

555

556

557

558

559

560

13 Figure Captions

Figure 1 Diagram of the signal processing steps of the atrial electrograms:1) St. Jude Ensite: left atrial Geometry isopotential map exported from Ensite Velocity System; 2) QRST subtraction: Electrograms using one ECG lead as reference; 3) FFT and DF detection: power spectrum of the current non-contact atrial signal and DF identification; 4) 3D and 2D DF/HDF maps: MATLAB reconstructed 3D Atrial geometry with color-coded DF/HDF and transformation to 2D uniform grid; 5) HDF maps identification: sequential 2D HDF maps used as input of the pattern extraction algorithm; 6) Pattern extraction: pattern extraction algorithm identifying recurrent spatial patterns.

Figure 2 A. The flowchart of the pattern extraction algorithm; **B.** all recurrent patterns of patient 6 with the 2D HDF maps involved in each pattern and the corresponding time windows numbers, color-coded 3D geometry showing the overlap of all the pattern windows.

Figure 3 A. Example of 3D HDF maps of the DP in patient 6; **B.** The time occurrences of the DP of each patient pre-/post- ablation (black: DP windows; grey: non-DP windows). Patients 4, 5 and 10 were in atrial flutter post ablation demonstrating a single DP.

Figure 4 A. 3D left atrial HDF maps in dominant pattern windows; **B. i.** Average mean DF of HDF regions in and outside DP windows before ablation; **ii.** Standard deviation of mean DF of HDF regions in and outside DP windows; **iii.** Average mean OI of HDF regions in and outside DP windows before ablation.

Figure 5 A. Example of the atrial segmentation and detection (top: Ensite; bottom: MATLAB reconstruction); **B.** Percentage of DP pattern occurrences of all patients at different atrial regions; **C.** Count of occurrences of DPs of all patients at different atrial regions.

Figure 6 A. DF values of HDF regions in 1st DP, 2nd DP, 3rd DP and non-DP for all patients (mean and standard deviation); **B.** OI values of HDF regions in 1st DP, 2nd DP, 3rd DP and non-DP for all patients (mean and standard deviation); **C.** Standard deviation of mean DF of HDF regions in 1st DP, 2nd DP, 3rd DP and non-DP for all patients (mean and standard deviation).

Figure 1 Li et al 2020

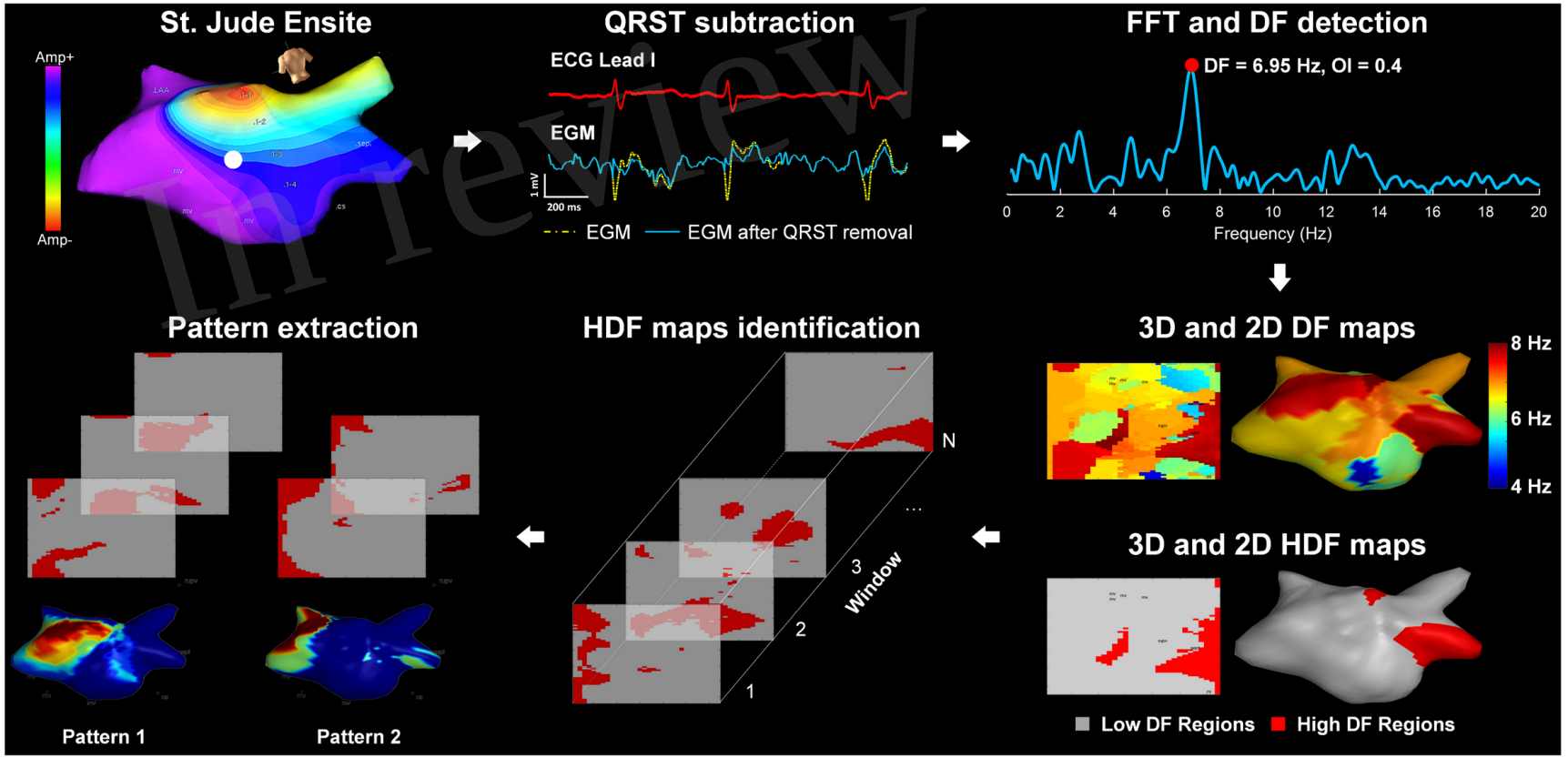

588

Figure 2 Li et al 2020

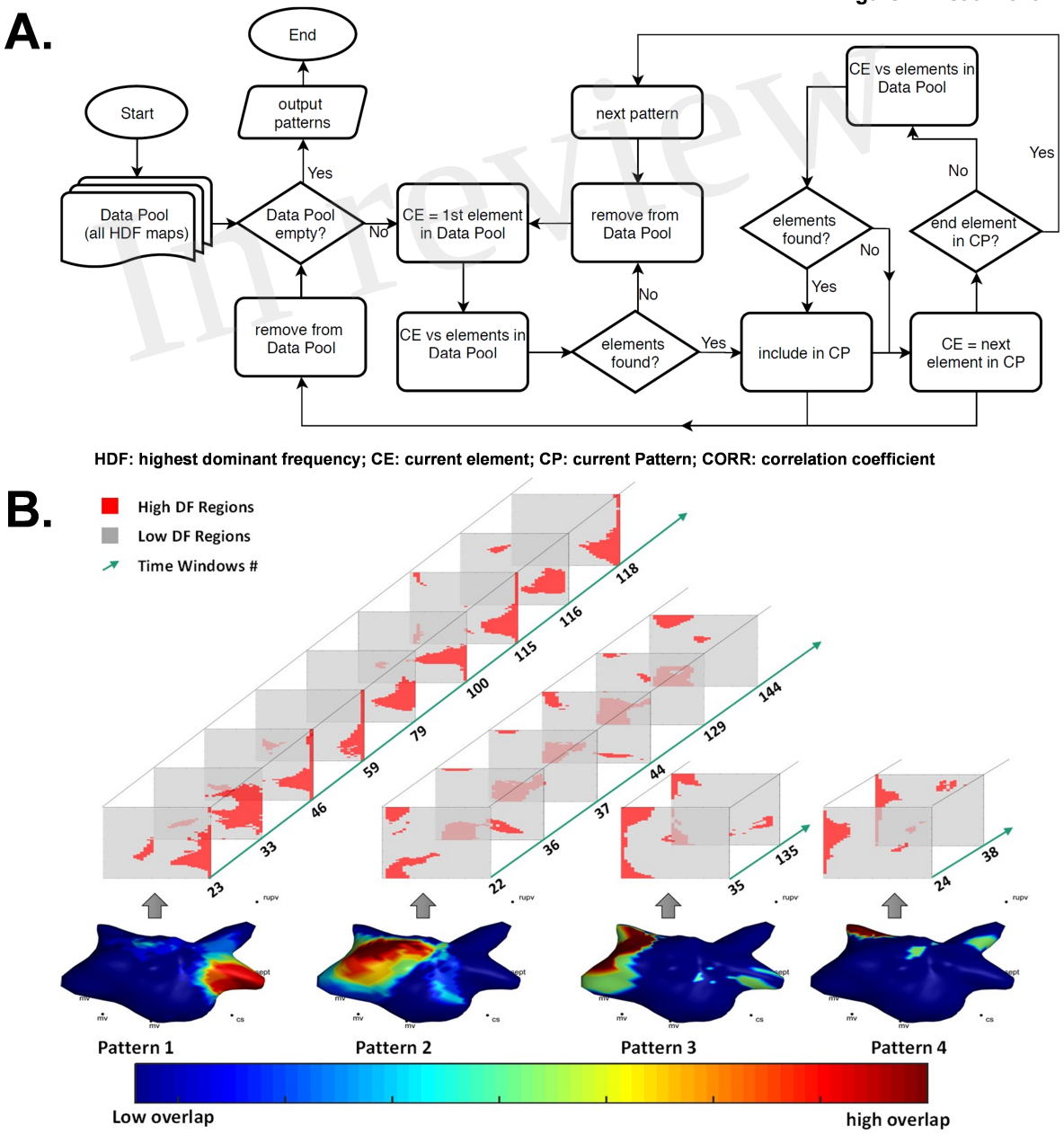

HDF: highest dominant frequency; CE: current element; CP: current Pattern; CORR: correlation coefficient

589

Figure 3 Li et al 2020

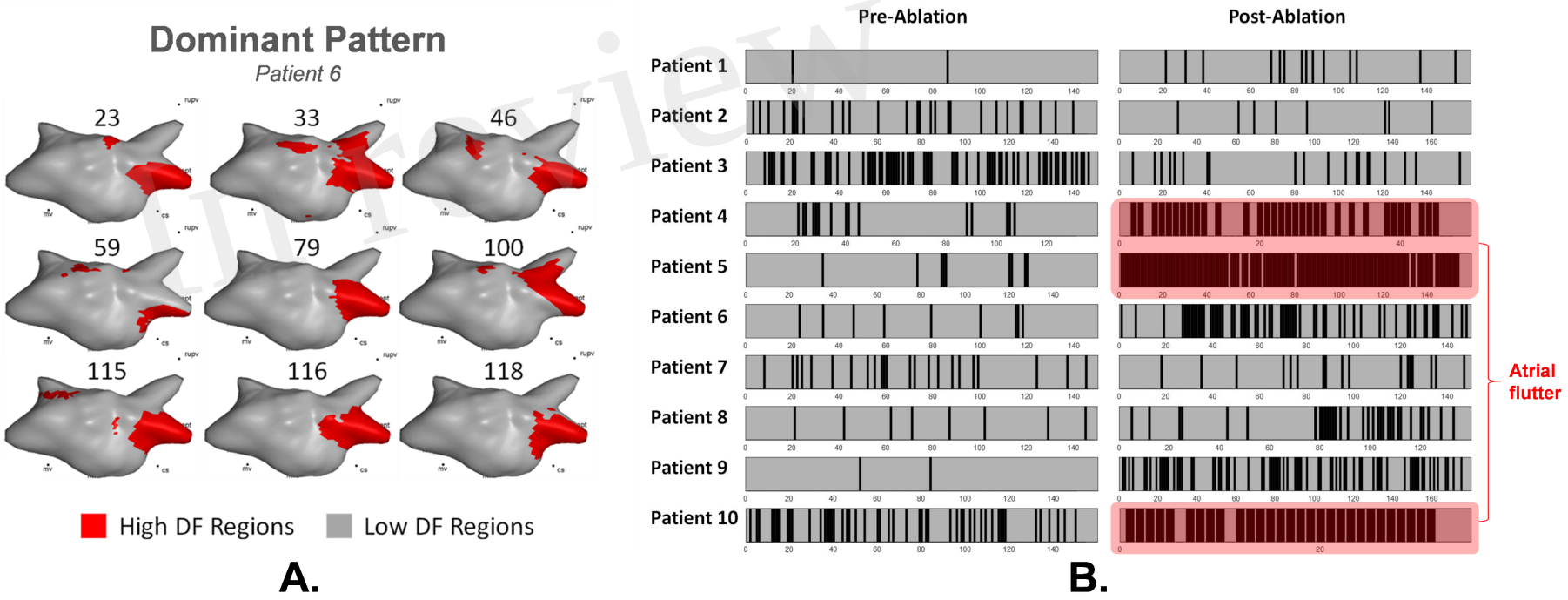

590

591

592

593

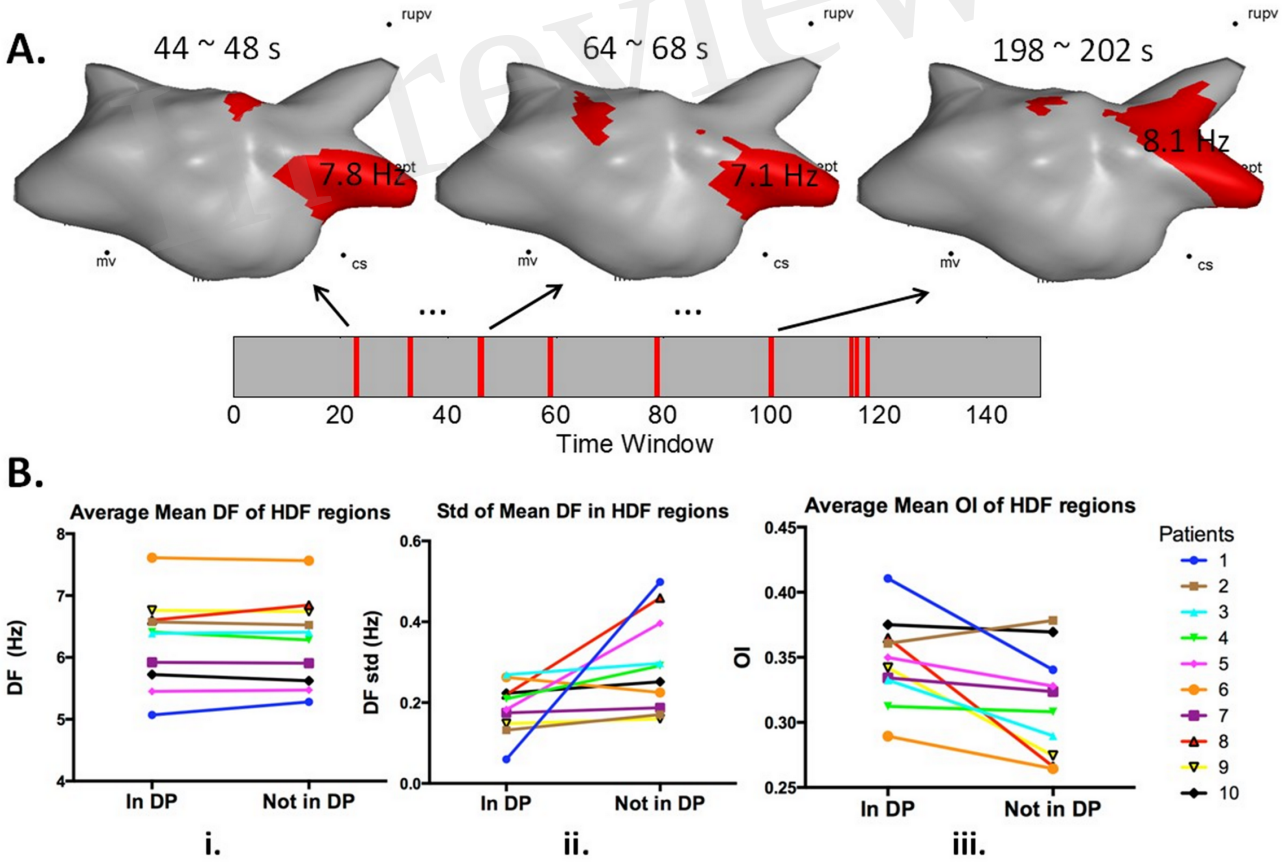

Figure 4 Li et al 2020

594

595

596

Figure 5 Li et al 2020

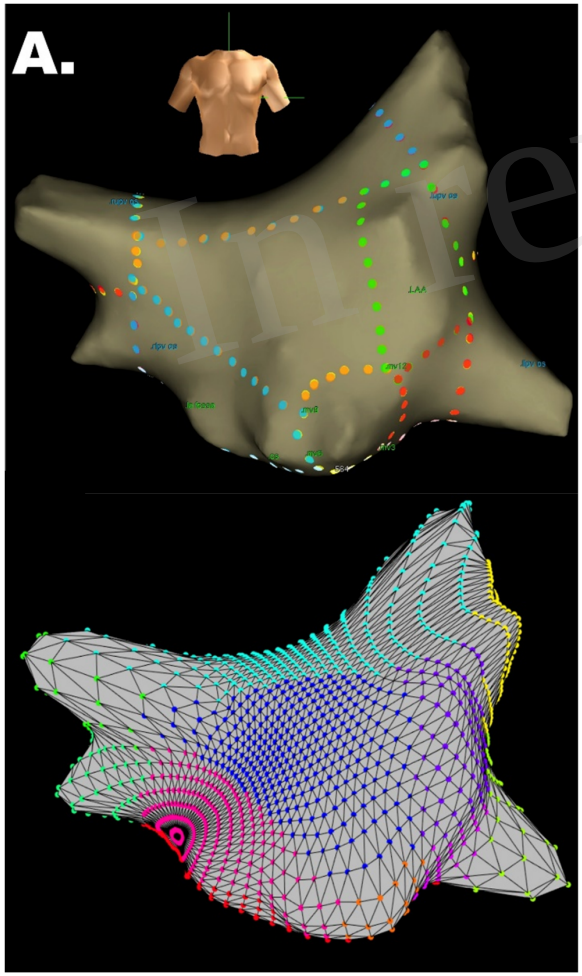

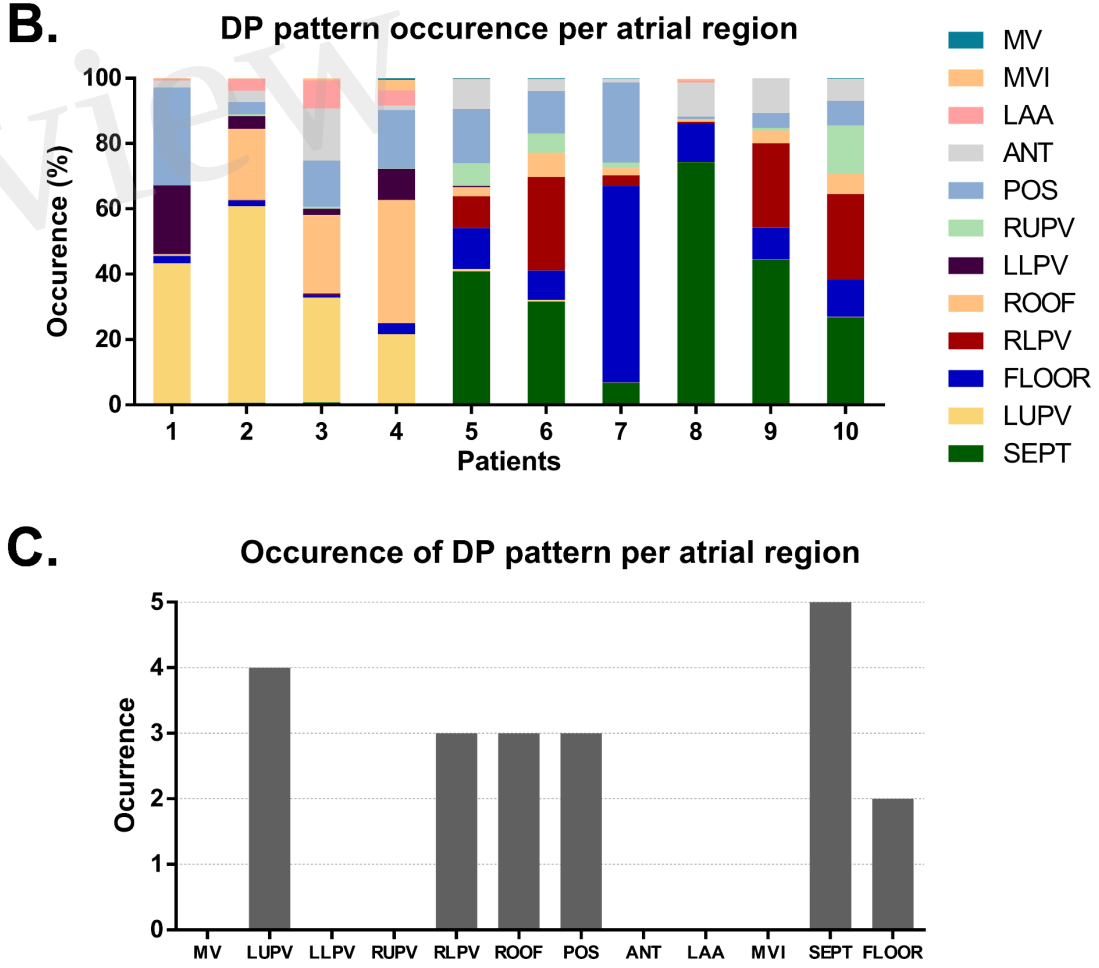

597

Figure 6 Li et al 2020

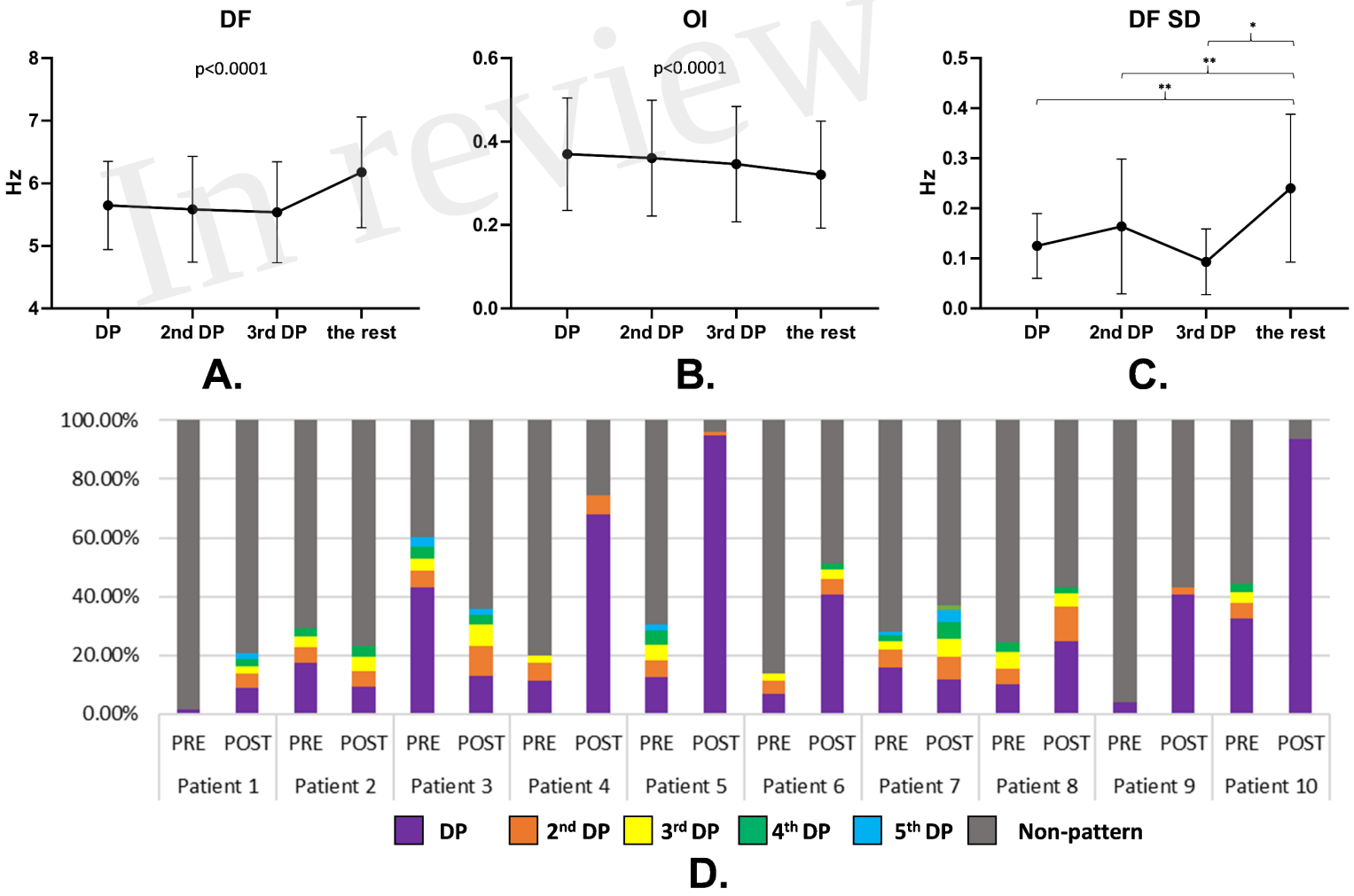

598

Figure 1.TIF

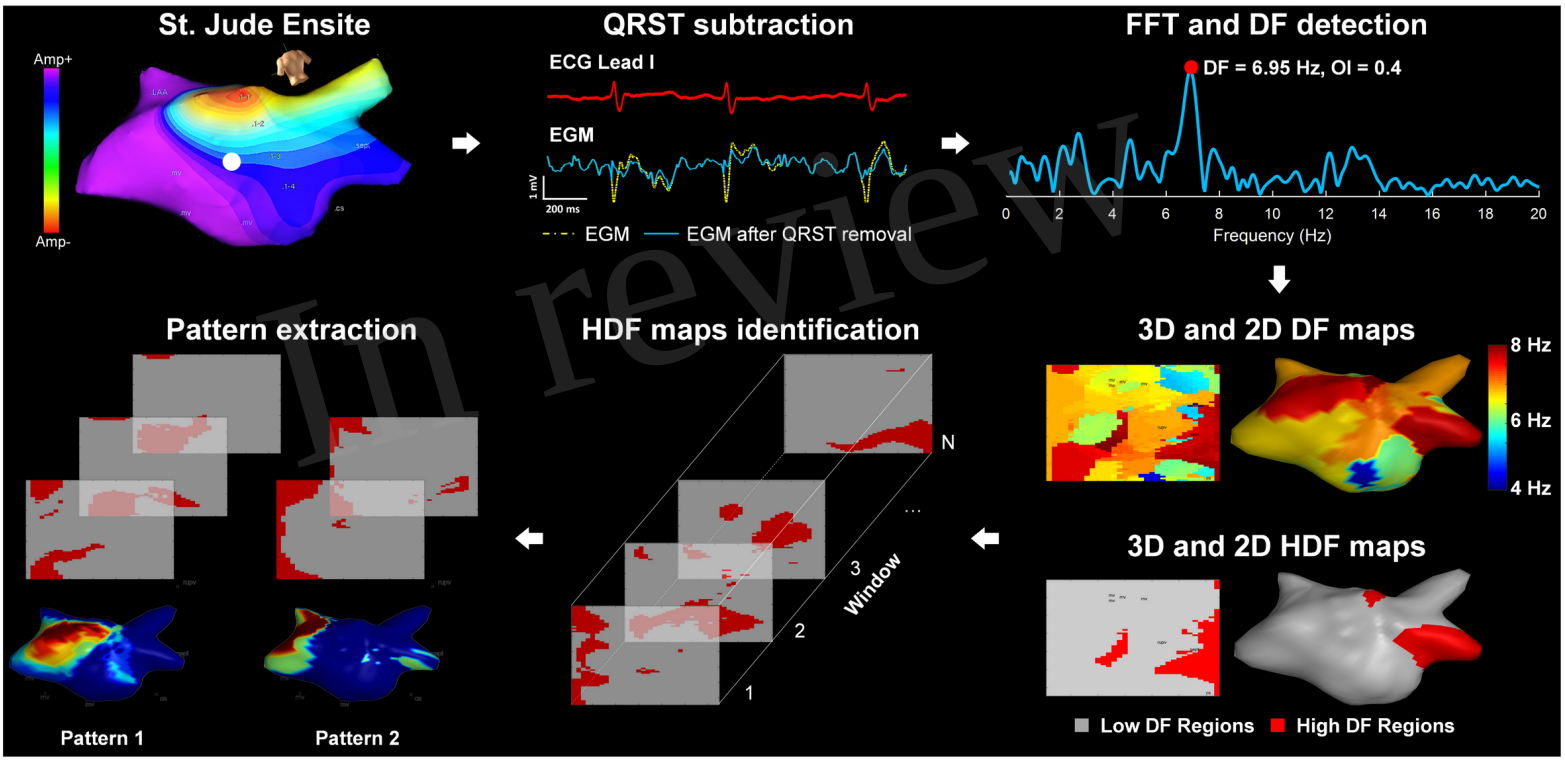
Figure 1 Li et al 2020
St. Jude Ensite
Amp+
Amp-
QRST subtraction
ECG Lead I
EGM
1 mV
200 ms
EGM
EGM after QRST removal
FFT and DF detection
DF = 6.95 Hz, OI = 0.4
0
2
4
6
8
10
12
14
16
18
20
Frequency (Hz)
3D and 2D DF maps
8 Hz
6 Hz
4 Hz
3D and 2D HDF maps
Low DF Regions
High DF Regions
HDF maps identification
N
3
2
1
Window
Pattern extraction
Pattern 1
Pattern 2
In review

Figure 2.TIF

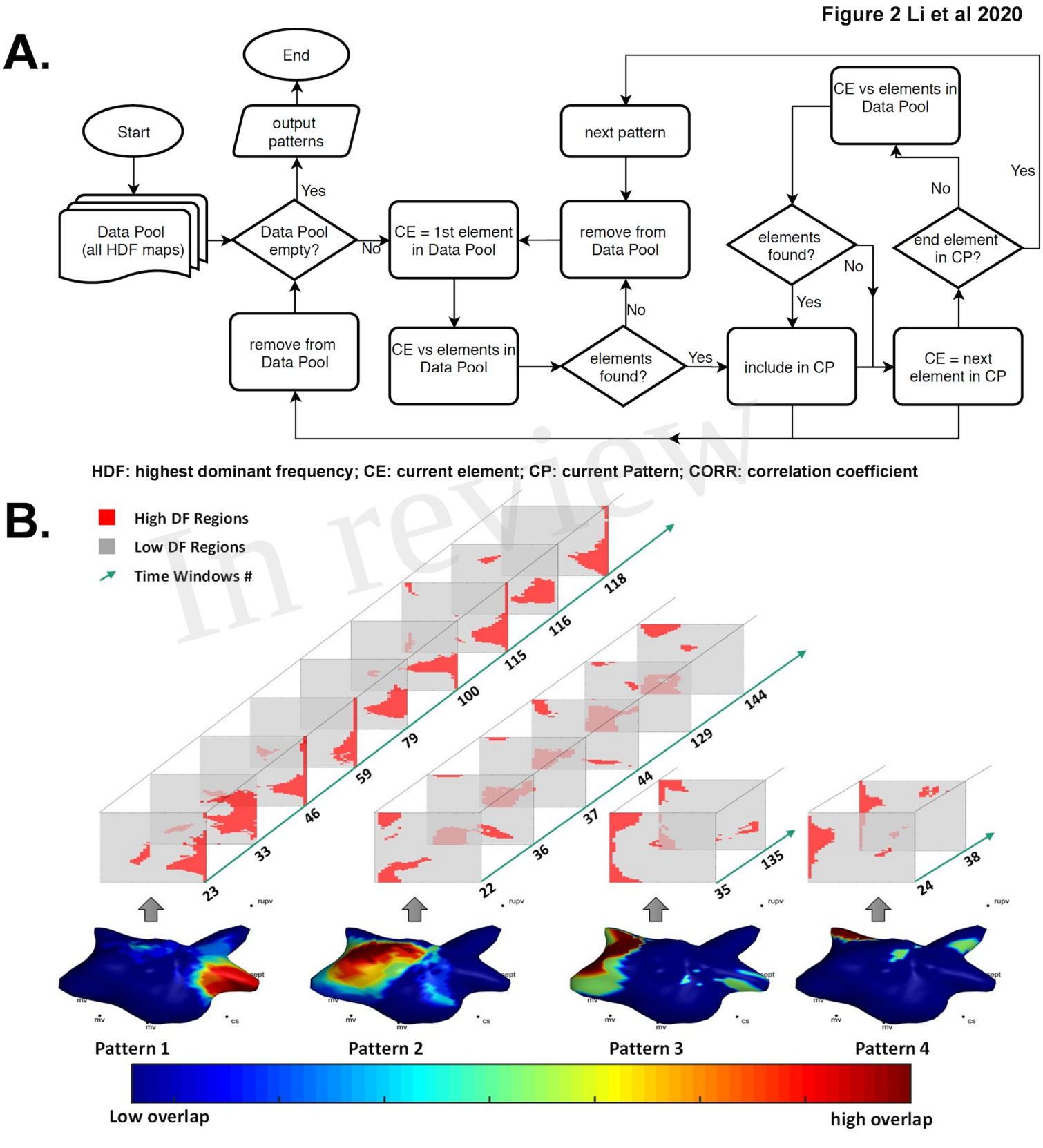

Figure 3.TIF

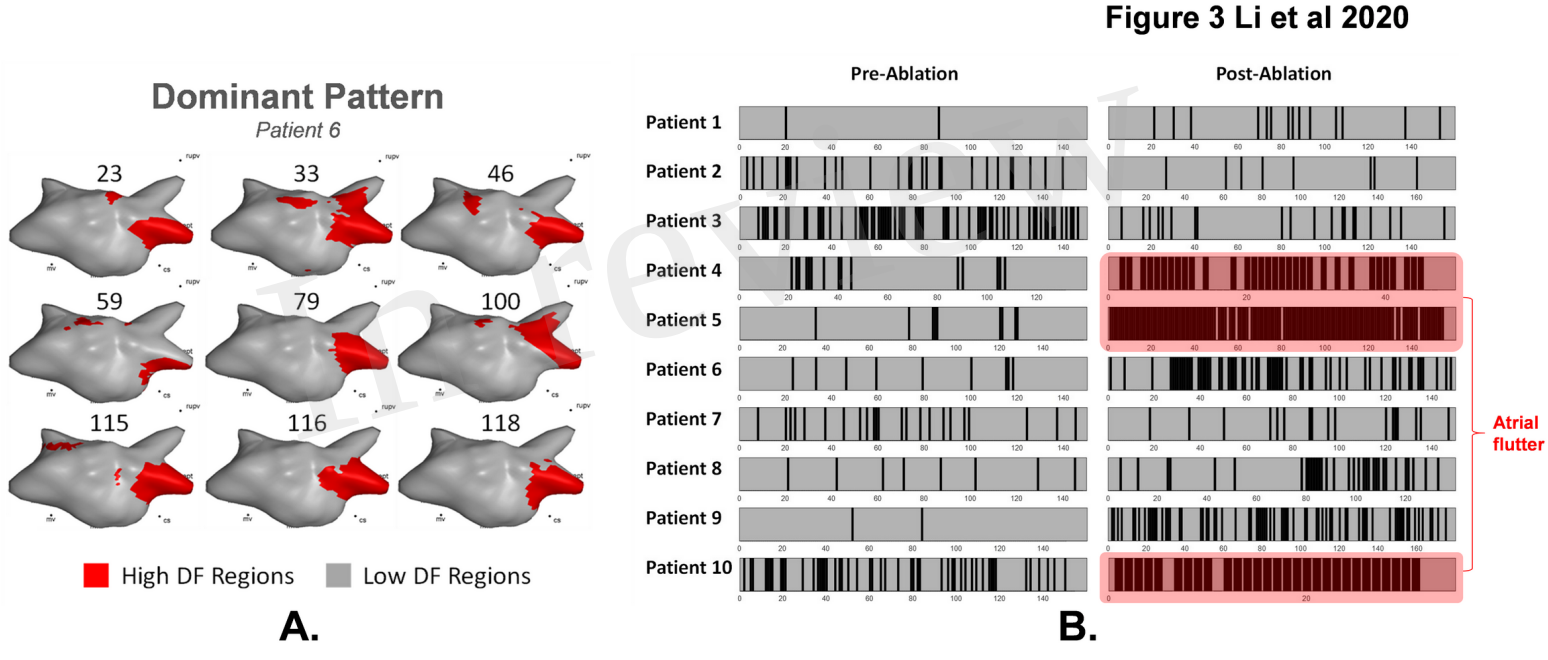
Figure 3 Li et al 2020
Dominant Pattern
Patient 6
23
33
46
59
79
100
115
116
118
High DF Regions
Low DF Regions
A.
Pre-Ablation
Post-Ablation
Patient 1
Patient 2
Patient 3
Patient 4
Patient 5
Patient 6
Patient 7
Patient 8
Patient 9
Patient 10
Atrial flutter
B.

Figure 4.TIF

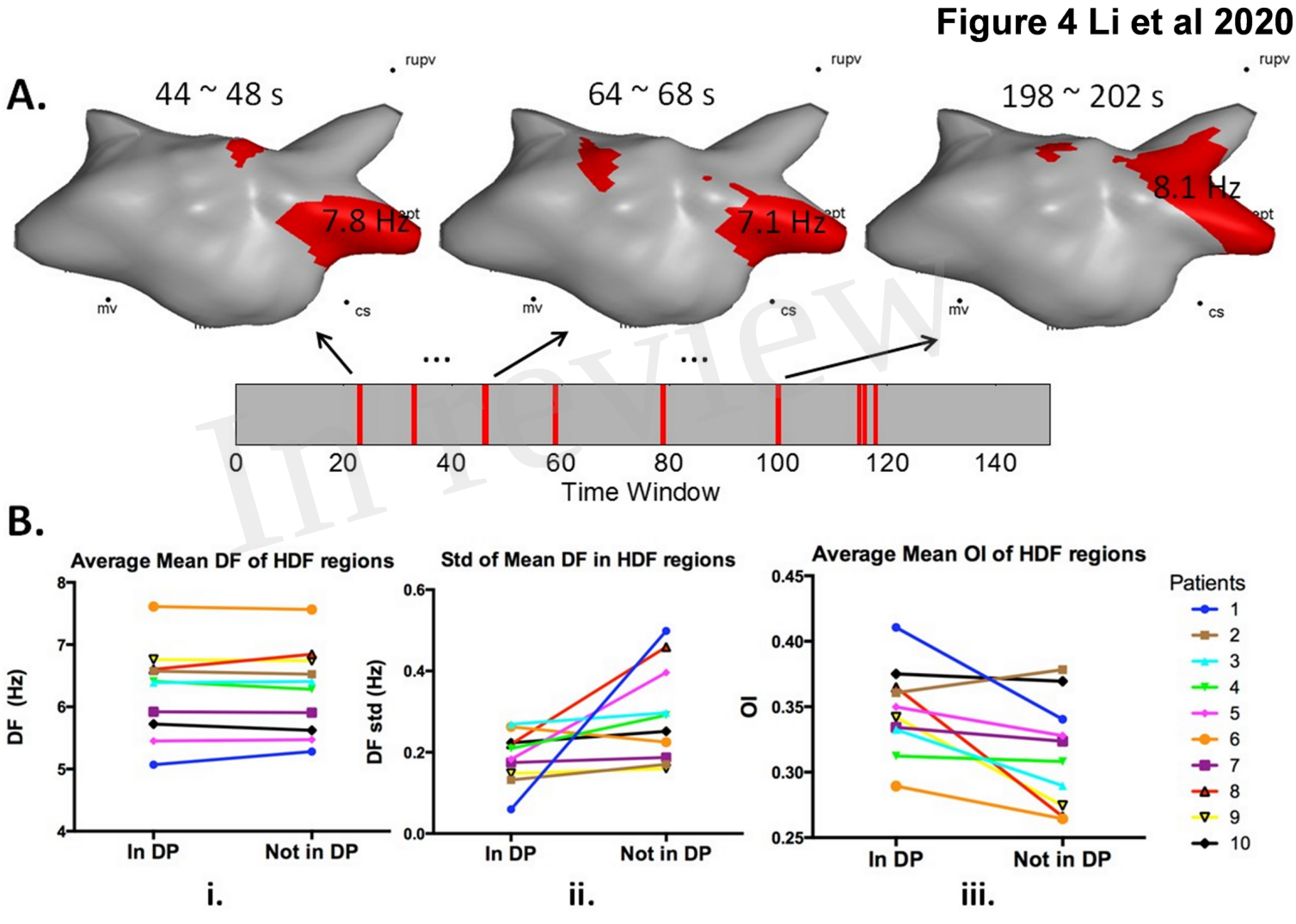

Figure 5.TIF

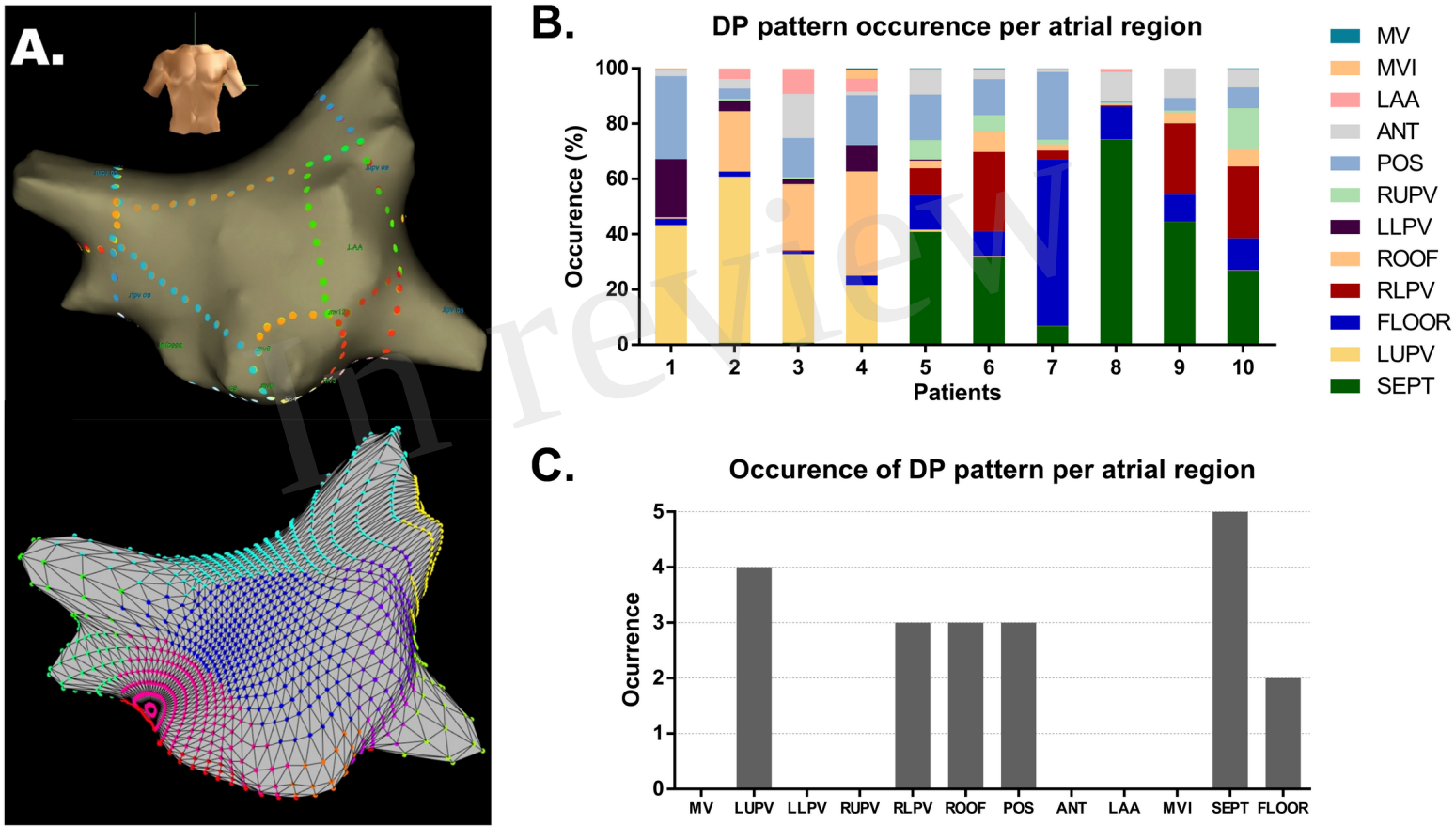

Figure 6.TIF